Evidence-based model for real-time surveillance of ARDS

Aline Taoum, Farah Mourad-Chehade, Hassan Amoud

Evidence-based Model for Real-time Surveillance of ARDS

Aline TAOUM[a,b,*], Farah MOURAD-CHEHADE[a], Hassan AMOUD[b]

[a] *Laboratoire de Modélisation et Sûreté des Systèmes*
Institut Charles Delaunay, Université de Technologies de Troyes, Troyes, France
[b] *Laboratory of Electronic Systems, Telecommunications and Networks*
Azm Platform for Research in Biotechnology and its Applications, EDST, Lebanese University, Tripoli, Lebanon

Abstract

Real-time health surveillance becomes important and necessary with the increase of the elderly population to preserve their quality of life. Real-time models aim to provide alerts before the severe illness occurs. Acute respiratory distress syndrome is a crucial disease of the respiratory system that threats the health of the elderly. This paper proposes a real-time model for the surveillance of ARDS based on belief functions theory. Non-invasive physiological signals are considered such as heart rate, respiratory rate, oxygen saturation and mean airway blood pressure. Different linear and nonlinear parameters are extracted from these signals; then a parameters selection procedure is performed to reduce their dimensionality. Afterwards, classifiers are constructed using parameters distributions defined in the evidence framework. Real-time prediction is then performed by combining all classifiers decisions. As results, high performances are obtained over the testing sets with performances of 77% and 71% for sensitivity and specificity, respectively.

Keywords: Acute respiratory distress syndrome; Evidence-based theory; Linear and nonlinear parameters; Real-time surveillance

1. Introduction

The elderly population is expected to increase from 962 million in 2017 to more than 2 billion by 2050 [1]. Older people are prone to many pathologies that reduce their autonomy and may threaten their lives leading to worldwide economic burden. The most known elderly-related pathologies are cardiovascular diseases, chronic respiratory diseases, neurological and mental disorders [2]. A real-time surveillance for elderly people helps to detect pathologies in advance. Thus it prevents its severity, shortens lengths of hospital stay and reduces mortality [3]. Real-time surveillance consists of

*Corresponding author
Email addresses: aline.taoum@utt.fr (Aline TAOUM), farah.chehade@utt.fr (Farah MOURAD-CHEHADE), hassan.amoud@ul.edu.lb (Hassan AMOUD)

continuous analysis of health-related data collected at a fixed time interval to reveal upcoming illness. It has been the subject of debate for many researchers [4, 5, 6]. In this paper, we present a real-time surveillance system for Acute Respiratory Distress Syndrome (ARDS).

ARDS is a severe disability of the respiratory system characterized by expanded pulmonary inflammation [7, 8]. It results in insufficiency of gas exchange with the blood, associated with high short-term mortality [9]. Over years, several definitions had been published until the Berlin Definition was proposed in 2012 [9, 10, 11]. Accordingly, ARDS is a hypoxemia that develops within one week of new respiratory inflammation symptoms or a known clinical insult. It is diagnosed using the ratio of the partial pressure of oxygen in the arterial blood (PaO_2) over the fraction of oxygen in the inspired air (FiO_2). Moreover, ARDS was classified as mild ($200\ mmHg < PaO_2/FiO_2 \leq 300\ mmHg$), moderate ($100\ mmHg < PaO_2/FiO_2 \leq 200\ mmHg$), or severe ARDS ($PaO_2/FiO_2 \leq 100\ mmHg$). All having a minimum positive end-expiratory pressure (PEEP) of 5 cm H_2O.

The risk of ARDS increases for patients who have undergone cardiac surgery or were hospitalized for severe health problems. Depending on the case, some patients were transferred from intensive care units (ICU) to wards or were completely discharged from hospitals. Therefore, the monitoring and early-identification of those patients is crucial in order to implement preventative measures. Generally, studies conducted on ARDS have used clinical variables to characterize it or to predict its onset. Some studies have investigated the risk factors associated with ARDS [12, 13], others have developed predictive algorithms for ARDS using clinical data of ventilated ICU patients, as in [14]. Other researchers have worked on mortality prediction related to ARDS [15, 16] or respiratory complications [17, 18].

Furthermore, data mining and machine learning techniques are widely adopted in biomedical applications to analyze, classify and predict medical data [19]. Classical machine learning techniques such as k-nearest neighbors [20], naive Bayes [21] and support vector machine [22] are applied on medical data to diagnose or predict a clinical abnormality in physiological signals. However, there is a lack in the literature of prediction models and real-time surveillance for ARDS.

This paper proposes a novel algorithm for predicting the occurrence of ARDS. A key point in this surveillance is considering multiple vital signs that are easy to collect[23, 24]. Identifying ARDS can be done using just one signal [25], but most of the serious diseases occur with concurrent irregularities in multiple vital signs [6]. Hence, in this study, physiological signals are analyzed continuously to identify the current health state of a patient. Multiple vital signs are used, that are the heart rate, the respiratory rate, the oxygen saturation and the mean airway blood pressure. Instead of using the whole signals, linear and non-linear parameters are extracted in real-time and the most informative ones are selected. After that, a prediction model based on evidence theory is defined in order to combine information of the extracted parameters and generate a decision regarding the health state of the patient in study. This model is constructed using the multi-parameter intelligent monitoring of intensive care II database.

The outline of the paper is as follows. In the next section, the patient extraction procedure is presented, and then the evidence-based method is introduced. Thereafter,

the results are illustrated and interpreted. Finally, a conclusion summarizes the paper and proposes some perspectives.

2. Materials

Subjects are extracted from the multi-parameter intelligent monitoring of intensive care II (MIMIC II) database. It contains two types of data: monitor waveforms and clinical data, collected over a seven years period. A detailed explanation of the database can be found in [26, 27]. In this study, the clinical database was considered first to select subjects, using the values of their PaO_2/FiO_2 ratios. Hence, an ARDS group is formed using the definition of both moderate and severe ARDS with $PaO_2/FiO_2 \leq$200 mmHg in addition to PEEP levels higher than 5 cmH_2O; while a non-ARDS group included subjects having mild and non ARDS patients with PEEP$<$5 cm H_2O. After that, the waveform database is matched to the selected subjects of the two groups, and their time series are extracted; that are the heart rate (HR), the respiratory rate (RR), the oxygen saturation (SpO_2) and the mean airway blood pressure (MABP). These time series have a frequency of 1 sample/min. This leads to 140 ARDS subjects and 135 non-ARDS subjects.

Among the ARDS subjects, there are 50 subjects that started their records after ARDS diagnosis. These subjects are irrelevant for this study and thus were eliminated. Other ARDS subjects started their records before the onset of ARDS but stopped before ARDS diagnosis; these subjects, of number equal to 18, are also eliminated. Therefore, only the 72 subjects having started records before the ARDS onset and last at least until ARDS occurrence are considered. After that, a preprocessing step was required to smooth the signals and remove the noise. Some subjects were removed due to noise or too short signals. This leads finally to 50 ARDS subjects. The non-ARDS group is then reduced to have equal number of subjects, leading to 50 non-ARDS subjects as well. Figure 1 illustrates an example of the four extracted time series for an ARDS subjects. Within the database of 100 subjects, a k-fold cross-validation technique is considered to set training databases and testing databases [28]. In the following, the terms *training set* and *testing set* would denote any training database obtained at any step of the cross-validation process with its corresponding testing database respectively.

3. Evidence-based surveillance approach

The method described in this paper is a real-time method that monitors the ongoing health state of patients using their vital signs. Let $x_{s,i}(\ell)$, $i = 1, \ldots, 4$, denote the four time series considered in this study for a subject s, recorded at time ℓ, and let t denote the real-time. Moreover, let $x_{s,i}(a : b) = (x_{s,i}(a), ..., x_{s,i}(b))$ be a segment of signal i for subject s going from time a to time b.

3.1. Description of the approach

The aim of this work is to set a model Ψ from a training set that distinguishes in real-time between subjects who are going to develop ARDS labeled "$+1$", and subjects who will not, labeled "-1". The model Ψ takes as input the collected signals

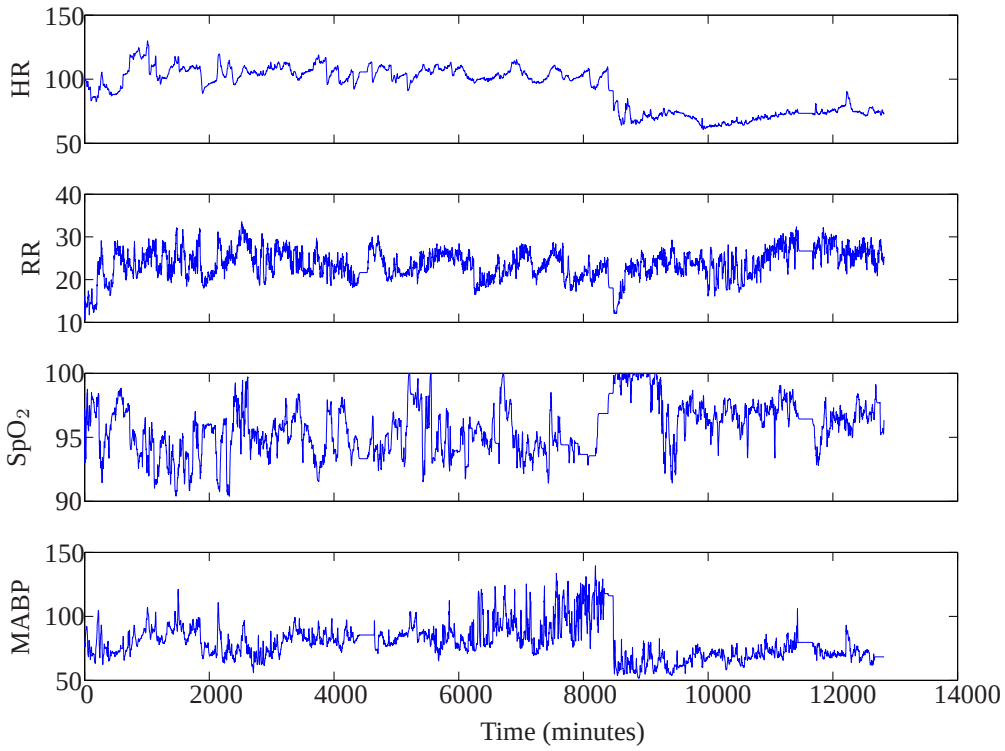

Figure 1: An example of the extracted time series for an ARDS subject

$x_{s,i}(1:t)$, going from the beginning of records until the real-time t, and yields as output a decision whether the subject in study is going to develop ARDS. Instead of using the whole signals, the proposed approach considers a fixed window of length τ taken at the end of the signals, leading to four segments $x_{s,i}(t-\tau+1:t)$ to be analyzed at each time t. The reason of analyzing the data of a window of length τ is to have fixed length signals in computations. Moreover, an abnormality is better and faster detected within a short segment, compared to the high length signal. The value of τ could be taken equal to 6, 12 or 24 hours. In this paper, it is obtained by an optimization over the training sets, as shown in the following. Then, a vector of parameters is extracted from these segments at real-time t. The beginning of the signals is yet needed to normalize these parameters. This vector of parameters is then used with the belief functions theory to assign evidence to each health state according to each parameter. The parameters are considered as sources of information, providing an evidence regarding each state of the patient at the given time. Thus, masses are assigned to each state "$+1$" and "-1" according to each parameter. The masses are obtained by means of mass functions defined using the parameters extracted from the training set at an earlier offline phase. The masses are then combined to assign a final mass to each state. A higher mass assigned to the state "$+1$" at time t means that the subject is predicted to develop ARDS in the future, whereas a higher mass to "-1" means that the ARDS is not yet predicted at the current time. Therefore, for a new test

subject given it signals in real-time, a decision will be made on its future health state at the earliest possible time.

3.2. Parameters Extraction

The first step of the prediction model is the extraction of parameters. Having a segment $x_{s,i}(t-\tau+1:t)$ from each signal at the real-time t, several linear and non-linear parameters are extracted as follows. In the following, t^- would denote the lower bound of the considered time interval, that is, $t^- = t-\tau+1$. For linear parameters, we consider:

- The mean defined as
$$\mu_{s,i}(t) = \frac{1}{\tau}\sum_{\ell=t^-}^{\ell=t} x_{s,i}(\ell);$$

- The standard deviation
$$\sigma_{s,i}(t) = \sqrt{\frac{1}{\tau}\sum_{\ell=t^-}^{\ell=t}(x_{s,i}(\ell)-\mu_{s,i}(t))^2};$$
The variance is equal to the total power of spectral analysis. Thus, it reflects all the cyclic components responsible for the variability in the data [29].

- The skewness known as the third moment. It measures the symmetry of the data and it is computed using
$$Sk_{s,i}(t) = \frac{\sum_{\ell=t^-}^{\ell=t}(x_{s,i}(\ell)-\mu_{s,i}(t))^3}{\tau\times\sigma_{s,i}^3(t)};$$
It has been proposed that asymmetric tails to the left shown by positive skewness or to the right with negative skewness reflect, respectively, the acceleration or deceleration capacity of the time series data, e.g. for heart rate signal, it is an approximate distinction of vagal and sympathetic effects on the cardiac modulations [30].

- The kurtosis that describes the shape of the probability distribution and is calculated using the fourth moment of the data,
$$Kt_{s,i}(t) = \frac{\sum_{\ell=t^-}^{\ell=t}(x_{s,i}(\ell)-\mu_{s,i}(t))^4}{\tau\times\sigma_{s,i}^4(t)}.$$
The kurtosis measures the concentration of the data around the mean and reflects the rigidity of the signal [31].

On the other hand, non linear parameters are also considered, such as:

- The sample entropy ($SampEn$), that illustrates the amount of complexity in data. It is easily applied to any type of time series, including physiological data such as heart rate variability and blood pressure variability [32, 33]. It is computed using the negative natural logarithm of the conditional probability that a segment of length N having repeated itself for u samples within a tolerance r will also repeat itself for $u + 1$ samples [34]. Hence, for the segment $x_{s,i}$ of length $N = \tau$, $SampEn$ is computed as follows,

$$SampEn_{s,i}(u, r, \tau, t) = -\ln\left(\frac{h_{s,i}(u+1, r)}{h_{s,i}(u, r)}\right),$$

where u is the length of sequences to be compared, r the tolerance for accepting and $h(u, r)$ is the number of pairs of patterns sequences of $x_{s,i}$ of length u whose distance is less than r.

- The detrended fluctuation analysis (DFA), that measures the scaling behavior of a segment [35]. It is defined by the short and long range scaling exponents DFA_1 and DFA_2. To perform detrended fluctuation analysis for a segment $x_{s,i}(t-\tau+1:t)$, the integrated series $y(u)$, $u = 1, \ldots, \tau$, is first computed

$$y(u) = \sum_{\ell=1}^{\ell=u} [x_{s,i}(\ell + t - \tau) - \mu_{s,i}(t)].$$

Then, $y(u)$ is divided into time segments of size n, and a local trend $y_n(u)$ is obtained by a least-squares line fit and subtracted from $y(u)$. The fluctuation $f(n)$ for segments of length n is calculated as follows:

$$f(n) = \sqrt{\frac{1}{\tau}\sum_{u=1}^{u=\tau}(y(u) - y_n(u))^2}.$$

The fluctuation $f(n)$ is computed for different segment sizes n, then a graph of $\log f(n)$ against $\log n$ is constructed. Finally, the scaling exponents DFA_1 and DFA_2 define, as their names denote, the slope of the relation between $\log f(n)$ and $\log n$ for ranges of low and high values of n.

DFA has been used to assess the self-similar correlations of the time series [36]. It has also been described as a measure of "roughness" in the signals, with higher scaling exponents representing a smoother time series [37].

Having the four measured signals, these computations lead to seven parameters per signal and thus twenty-eight parameters, for each subject s at each time t. Let $p_{s,j}(t)$, $j = 1, ..., 28$, denote these parameters. For many health conditions, the trends in vital signs differ among patients. Thus, normal is a relative state for each patient, that differs with age, weight, medical history, etc. Hence, instead of using the raw values of the parameters, a normalization phase is performed according to each patient. Therefore, a first segment of length τ is considered from each signal, $x_{s,i}(1 : \tau)$. It corresponds to the initial state of the patient that is assumed to be its stable one.

Then, the different parameters are computed for the initial segments. Let $p_{s,j}^{(0)}$ denote their initial values. Then, for each real-time measurement, the obtained parameters are normalized, by computing their ratio to the parameters of the first segment $p_{s,j}(t)/p_{s,j}^{(0)}$. In the following, $p_{s,j}$ would denote the normalized parameter, for simplicity.

Note that, a parameter selection would be performed in the offline phase using the training set to keep only informative one. More details are given in Section 3.4. In the following, let J be the set of indices of the selected parameters, and thus $p_{s,j}(t)$, $j \in J$, are the normalized parameters extracted at real-time t from a subject s signals.

3.3. ARDS prediction with Belief functions

The theory of belief functions, also called Dempster-Shafer theory, is introduced for the analysis of imperfect information[38, 39]. This theory makes it possible to illustrate the uncertainty and imprecision of information. It also takes into account ambiguities and conflicts between sources. The belief functions theory operates on a frame of discernment Ω which consists of a finite set containing mutually exclusive propositions. In this study, there are two groups of subjects, ARDS labeled "$+1$" and non-ARDS labeled "-1". Then $\Omega = \{+1, -1\}$. Let 2^Ω be the set of all possible subsets of Ω, it is then defined by:

$$2^\Omega = \{\emptyset, \{+1\}, \{-1\}, \{+1, -1\}\}.$$

While $\emptyset$ denotes that the state of the subject is neither ARDS, nor non-ARDS, which means impossibility, $\{+1, -1\}$ denotes ignorance and thus ambiguity.

3.3.1. Basic concept

The main concept relies on the modeling of the evidence provided by the extracted parameters. Information given by a source, that is a parameter, can be represented by a *basic belief assignment* (BBA), also named mass function [40]. Let $m_j(\cdot)$ be the mass function associated to the parameter p_j. Then, $m_j(\omega, s, t)$ reflects the strength of evidence supporting a subset $\omega \in 2^\Omega$ according to the value of the parameter p_j at time t. In other words, $m_j(\omega, s, t)$ represents the part of evidence saying that the state of the subject s falls in ω at time t. The mass function should have the following properties $\forall s, t$:

$$\begin{cases} m_j(\emptyset, s, t) = 0, \\ m_j(\omega, s, t) \to [0, 1], \text{for } \omega \in 2^\Omega, \\ \sum\limits_{\omega \in 2^\Omega} m_j(\omega, s, t) = 1. \end{cases} \tag{1}$$

In order to construct the mass functions related to each parameter, the training sets are considered. For ARDS subjects of a given training set, the last segments of their signals are used to compute their parameters $p_{s,j} = p_{s,j}(T_s)$, T_s being the length of the signals of an ARDS subject s. The reason of this choice is that the end of the signals precedes directly the occurrence of ARDS and thus contains mostly its instability. For non-ARDS subjects, the more the segments approaches the beginning of the signals, the more we are sure of the stability of the subject, since it is possible that a subject labeled non-ARDS develops the ARDS after recordings. Then, the parameters of non-ARDS are computed using segments selected from the wholly beginning of the signals,

following the first segments. Let S_{+1} and S_{-1} be the sets of indices of ARDS and non-ARDS subjects of the training set respectively. Then, normalized parameters databases $p_{s,j}$, $s \in S_{+1}$, and $p_{s',j}$, $s' \in S_{-1}$, are obtained. Afterwards, for a parameter type j, the pdfs are estimated using (1) only ARDS parameters values $p_{s,j}$, $s \in S_{+1}$, (2) only non-ARDS values $p_{s',j}$, $s' \in S_{-1}$ and (3) parameters of both classes $p_{s,j}$, $s \in S_{+1} \cup S_{-1}$. Let $Q_{j,\{+1\}}(\cdot)$, $Q_{j,\{-1\}}(\cdot)$ and $Q_{j,\{+1,-1\}}(\cdot)$ denote the estimated pdfs. These distributions could be obtained by fitting the histograms of the parameters to all the classical distributions. Then, in the online phase, having a computed parameter $p_{s,j}(t)$ at the real-time t, the mass assigned to each subset of 2^{Ω} is given by

$$m_j(\omega, s, t) = \frac{Q_{j,\omega}(p_{s,j}(t))}{\sum\limits_{\omega' \in 2^{\Omega}, \omega' \neq \emptyset} Q_{j,\omega'}(p_{s,j}(t))}, \omega \in 2^{\Omega}, \omega \neq \emptyset, \tag{2}$$

whereas $m_j(\emptyset, s, t) = 0$. Figure 2 illustrates an example of such a computation. The plot shows the distributions of the normalized standard deviation of respiratory rate signals parameter for ARDS subjects of a training database in straight thick line, the one for non-ARDS subjects in dashed line and the one of all subjects in straight thin line. Moreover, the plot shows the mass assignment for two new parameter values $p_2^{(1)}$ and $p_2^{(2)}$. The first parameter value falls in the distribution of ARDS subjects and the second is in the middle of ARDS and non-ARDS distributions. When assigning the masses of each value from Eq. (2), the assigned mass of $p_2^{(1)}$ from $Q_{j,\{+1\}}$ is higher than those of $Q_{j,\{-1\}}$ and $Q_{j,\{+1,-1\}}$. Thus, the decision obtained from the parameter $p_2^{(1)}$ is the state of $\{+1\}$. On the other hand, for parameter $p_2^{(2)}$, the distributions of $\{+1\}$ and $\{-1\}$ are too close, leading to similar masses from both. However, higher mass is associated in this case to the distribution of $\{+1, -1\}$, thus introducing the ambiguity of such case. The mass assigned to $\{+1, -1\}$ is higher than those of $\{+1\}$ and $\{-1\}$ in all the cases where these distributions are too close. This figure illustrates the effectiveness of the evidence-theory concept by inserting ambiguities when dealing with close data and thus avoiding erroneous decisions.

3.3.2. Discounting

Since we are working on parameters extracted from human bodies, the information cannot be completely reliable. Hence, a discounting operation is needed to take into consideration the reliability of the information provided by each parameter [39, 41]. This operation transforms each mass function to a less informative one, based on the degree of reliability of the source. Moreover, in this approach, it is possible to estimate its reliability according to each state, leading to a contextual discounting [42, 43]. Let $\beta_{j,\{+1\}} = 1 - \alpha_{j,\{+1\}}$ and $\beta_{j,\{-1\}} = 1 - \alpha_{j,\{-1\}}$ be the degrees of reliability of a parameter p_j knowing that the true state is " $+1$" and " -1" respectively. Then the

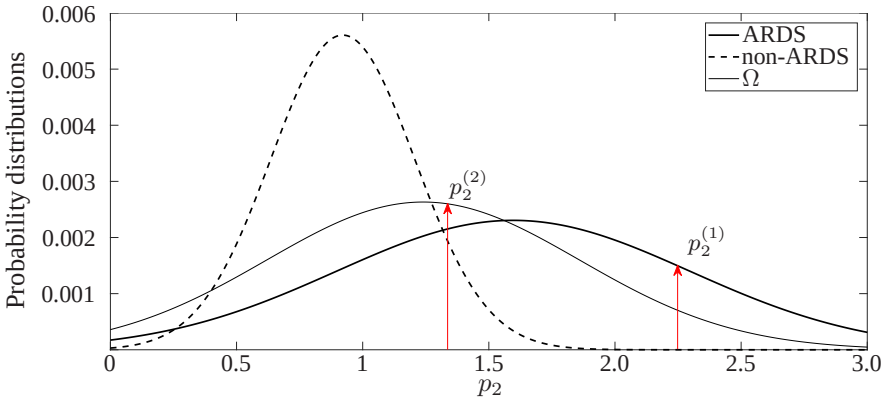

Figure 2: Mass assignment of new computations in the case of the normalized standard deviation of respiratory rate signals.

discounted mass function ${}^{\alpha}m_j$ assigned to p_j is given by

$$\begin{cases} {}^{\alpha}m_j(\{+1\}, s, t) = \beta_{j,\{-1\}} m_j(\{+1\}, s, t), \\ {}^{\alpha}m_j(\{-1\}, s, t) = \beta_{j,\{+1\}} m_j(\{-1\}, s, t), \\ {}^{\alpha}m_j(\Omega, s, t) = m_j(\Omega, s, t) + \alpha_{j,\{-1\}} m_j(\{+1\}, s, t) + \alpha_{j,\{+1\}} m_j(\{-1\}, s, t), \\ {}^{\alpha}m_j(\emptyset, s, t) = 0. \end{cases} \tag{3}$$

The error rates $\alpha_{j,\{+1\}}$ and $\alpha_{j,\{-1\}}$ could be estimated using the distribution functions $Q_{j,\omega}$. Knowing that a subject s state is equal to " $+1$", an error is made in evidence assignment if a higher mass is given to any subset of Ω other than $\{+1\}$. It is also the same for $\{-1\}$. Then, $\alpha_{j,\omega}$, $\omega = \{+1\}$ or $\{-1\}$, is computed for all parameter values, where $Q_{j,\omega}(p)$ is less than any $Q_{j,\omega'}(p)$, for $\omega' \neq \omega \in 2^{\Omega}$. Therefore, it is defined as follows:

$$\alpha_{j,\omega} = \epsilon_{j,\omega} = \int_{D_{j,\omega}} Q_{j,\omega}(p) dp, \tag{4}$$

where $D_{j,\omega} = \{p | Q_{j,\omega}(p) < Q_{j,\omega'}(p), \forall \omega' \in 2^{\Omega}, \omega' \neq \omega\}$.

3.3.3. Combination

Once the discounted masses of the different parameters are computed, they can be combined using the normalized conjunctive rule of combination from the Dempster-Shafer theory. By doing this computation, one obtains a more informative mass function, leading to more efficient estimation. The combination of these masses is denoted by $\oplus$ and defined by the following equation:

$$m_{\oplus}(\omega, s, t) = \frac{\sum\limits_{\cap \omega'^{(j)} = \omega} \prod\limits_{j \in J} {}^{(\alpha)}m_j(\omega'^{(j)}, s, t)}{1 - \sum\limits_{\cap \omega'^{(j)} = \emptyset} \prod\limits_{j \in J} {}^{(\alpha)}m_j(\omega'^{(j)}, s, t)}. \tag{5}$$

3.3.4. Decision making

Finally, to make a decision on the health state of a subject s, the mass function $m_{\oplus}$ defined on Ω is transformed to a probability measure over the singletons with the pignistic transformation defined by:

$$BetP(\omega, s, t) = \sum_{\omega' \in 2^{\Omega}, \omega \subseteq \omega'} \frac{m_{\oplus}(\omega', s, t)}{\mid \omega' \mid}, \forall \omega \in \Omega, \tag{6}$$

for $\omega = \{+1\}$ or $\{-1\}$. In this way, the final mass of $\{+1, -1\}$ subset is divided between $\{+1\}$ and $\{-1\}$. The state having the highest pignistic level is selected for each subject at every time t. Thus, a decision is made over the health state of subject s whether he will develop ARDS based on its recordings, and an alert is generated for a positive decision.

To make a final decision from the real-time analysis about the health state of a patient, it is also possible to wait for successive positive decisions. Here, a threshold must be defined as being the number of successive ARDS decisions needed to decide if the patient is going to develop ARDS. This is done by applying the algorithm iteratively on the total length of the signals s of the training set, then different numbers of successive positive decisions are considered and the performance indexes are computed for each number, that are the sensitivity (Se) and specificity (Sp) indexes, also called true positive rate and true negative rate, respectively. The threshold of successive ARDS decisions is obtained thereafter by maximizing the Youden index, $Youden = Se + Sp - 100$, over all the considered numbers.

Waiting for successive positive estimations overcomes detection of islolated abnormalities and leads to a higher specificity of the algorithm.

3.4. Selection of parameters

Instead of considering all the extracted parameters in the model, it is relevant to select the most informative ones with less error rates. This part of the algorithm consists of ranking the parameters according to their error rates and then performing a sequential forward selection (SFS) of parameters [44]. Hence, an error rate ϵ_j is computed for each parameter p_j, which is the average of conditional errors, $\epsilon_j = (\epsilon_{j,\{+1\}} + \epsilon_{j,\{-1\}})/2$. The conditional errors $\epsilon_{j,\omega}$ are computed using (4). A global ranking of parameters is performed. Parameters from all signals are ordered from the lowest error obtained to the highest one.

Once the parameters are ranked, a sequential forward selection procedure is performed. One parameter is added at a time and performance indexes of the model are computed. For each added parameter, the belief model is applied in real-time for all the subjects of the training set and a decision is generated for each of them. The sensitivity and specificity indexes are computed. Thereafter, A curve is plotted and updated at each iteration illustrating the sum of the performance indexes obtained versus the number of parameters. Whenever a new value added to the curve shows a decrease in the performance higher than a value ε, the SFS procedure ends and the parameters obtained are maintained.

In addition, in order to take into consideration the dependence of the parameters, the correlation between the added parameter and the existing parameters is tested and

Table 1: The most significant parameters for each signal, parameters having a p-value < 0.02 are shown. Mean $\pm$ standard deviation are shown for each parameter.

Signal	Parameters	ARDS group	non ARDS group
HR	$mean$	1.0297 ± 0.1439	1.0218 ± 0.0935
	Sk	-1.875 ± 6	-3.3629 ± 31.2769
	Kt	1.0628 ± 0.4082	1.2803 ± 0.6892
	$SampEn$	1.2277 ± 0.6079	1.0231 ± 0.1371
RR	σ	1.6226 ± 1.4729	0.9209 ± 0.2851
	Sk	-0.8592 ± 10.6885	1.0231 ± 3.3186
	Kt	1.0172 ± 0.5052	1.3381 ± 1.2061
	$SampEn$	1.4088 ± 0.5191	1.0281 ± 0.2
SpO$_2$	Sk	0.6881 ± 4.0655	3.1707 ± 14.2335
	Kt	1.0871 ± 0.5252	1.0907 ± 0.8359
	$SampEn$	1.2836 ± 0.6092	1.5598 ± 0.982
	DFA_1	0.8678 ± 0.1777	1.0172 ± 0.2767
	DFA_2	1.0289 ± 0.1349	1.0194 ± 0.0667
MABP	μ	1.0262 ± 0.1246	0.9868 ± 0.072
	Sk	0.6396 ± 1.6238	0.5796 ± 8.2055
	DFA_1	0.9432 ± 0.1459	1.0743 ± 0.3192
	DFA_2	0.9985 ± 0.0178	1.0022 ± 0.0397

compared to the selection procedure alone. If any correlation coefficient between the parameters presents a p_value ≤ 0.05 then the parameter is considered correlated with an existing one, thus it is eliminated from the selection procedure.

4. Results

As mentioned above, two types of parameters were extracted from each time series. Linear parameters are the mean μ, the standard deviation σ, the skewness Sk and the kurtosis Kt. Non linear parameters are the sample entropy $SampEn$, and both factors from the detrended fluctuation analysis DFA_1 and DFA_2. For sample entropy, the value of u is taken equal to 5, and r equals 0.2, as mentioned in [45]. For the detrended fluctuation analysis, DFA_1 is calculated between the range $n = 4$ and $n = 16$ and DFA_2 is calculated between $n = 16$ and $n = 64$, as shown in [35]. The results are obtained by a 5 fold cross validation repeated 10 times. For the illustration of the approach, presented in Sections 4.1, 4.2 and 4.4, only one training and one test sets are considered, then all the sets are considered for the performance evaluation in Section 4.5.

4.1. Statistical analysis

First, a statistical analysis is performed to identify parameters that show a significant difference between ARDS and non-ARDS groups. For each parameter, values were compared between both groups using the two-sample F-test. A p-value < 0.02 was considered as significant. Results are presented in Table 1. Different linear and

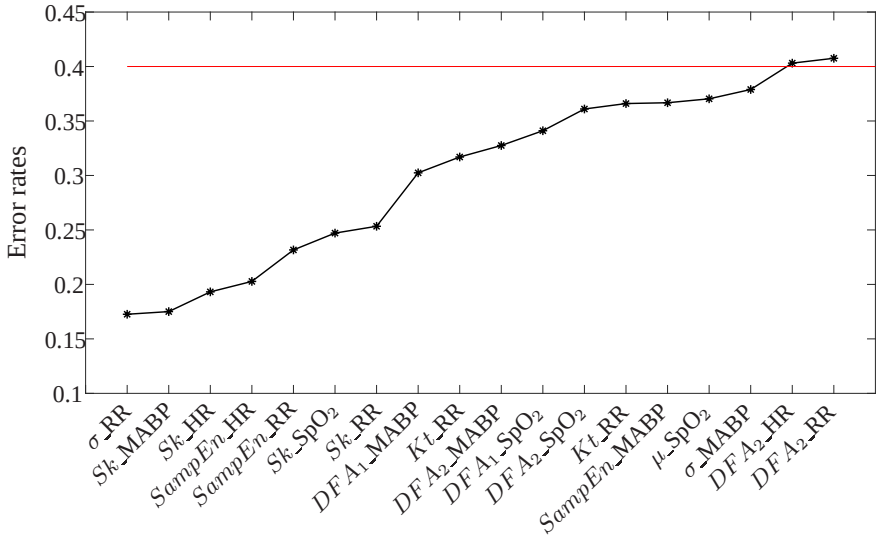

Figure 3: Ranking of parameters according to error rates. Only parameters having an error lower than 0.4 are included in the figure.

non-linear parameters for each signal has shown significant difference between groups. It can be noted from the table that distributions of non ARDS group are more asymmetric than ARDS group for all the signals from the values of skewness. In addition to being asymmetric, kurtosis shows that distributions of non ARDS group for HR, RR and SpO_2 have heavy tails. Moreover, RR's distribution is widely spread in ARDS group according to σ. For ARDS group, sample entropy is higher in HR and RR signals; while it is lower in SpO_2. Detrended fluctuation analysis factors are generally higher in non ARDS group for SpO_2 and MABP signal.

4.2. Parameters Selection

Since there is a high number of parameters, a ranking of these parameters based on the error rates is performed. The ranking is illustrated in Figure 3. Parameters having error rates higher than 0.4 are not presented. The results obtained from the error rate ranking in the figure are confirmed from the statistical analysis shown in Table 1. As shown, most of the parameters that have low errors in Figure 3 also showed a significant difference in the table. This figure shows that the standard deviation extracted from RR signals presented the lowest error rate among all parameters extracted from the four signals, thus ranking at the top.

From these ranked parameters, a sequential feature selection is considered to reduce the input vector of the belief computations. Figure 4 illustrates the selection procedure on the training set for both cases with and without correlations. The plot shows the accuracy as a function of the indicators of the ranked parameters. The accuracy is defined by the proportion of correctly identified subjects among the total number of subjects. A marker is placed on the curves when a parameter is selected. Starting with σ from RR, the parameters presented in Figure 3 are added sequentially until

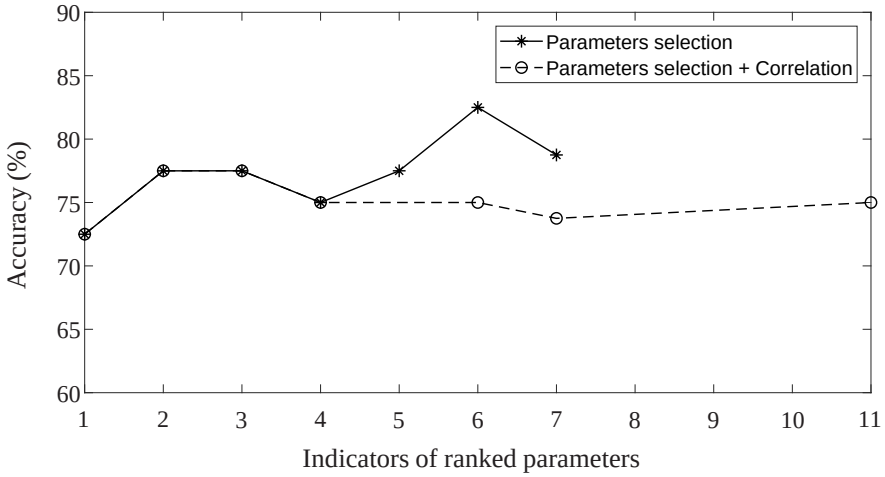

Figure 4: The parameters selection procedure using the simple procedure and the correlation extension procedure.

the accuracy decreases more than $\epsilon > 5\%$. For the correlation study, if a parameter shows a correlation with any existing parameter with a p_value lower than 0.05 it is excluded from the selection. The simple selection procedure finished on the insertion of the seventh parameter that is Sk from RR. Thus, six parameters are selected in the simple SFS procedure which are Sk and $SampEn$ from HR, σ and $SampEn$ from RR, Sk from both SpO_2 and MABP. However, there is no decrease in the accuracy of the model in the correlation study but the accuracy is lower than that obtained from the simple selection.

4.3. Selection of the alert generation threshold

In order to make a decision on the health state of a new test subject, a threshold must be defined from the training set. Therefore, we sweep the value of successive decisions on the interval $[1, ..., 30]$ hours and the performances Se and Sp are computed. The threshold that maximizes the Youden index is then considered. Figure 5 illustrates the ROC curve of the proposed algorithm by taking the fusion of the first six parameters obtained in the previous section. The plot shows that the optimal cut-off value is obtained for threshold $= 20$ hours with $Se = 81.4\%$ and $Sp = 83.78\%$.

4.4. Selection of window size

As described in the real-time model we have used a fixed-length window for extracting the parameters vector for all subjects. Thus, the selection of the size of the window is important in this study. A short window may not contain enough information and a long window may eliminate an abnormal change in the signal. Different window sizes are evaluated in this study, values are considered in the range $[4, 6, \ldots, 24]$ hours. Figure 6 illustrates the accuracy for each window size (in hours) as well as the number of selected parameters and the threshold shown as a couple (number of parameters,

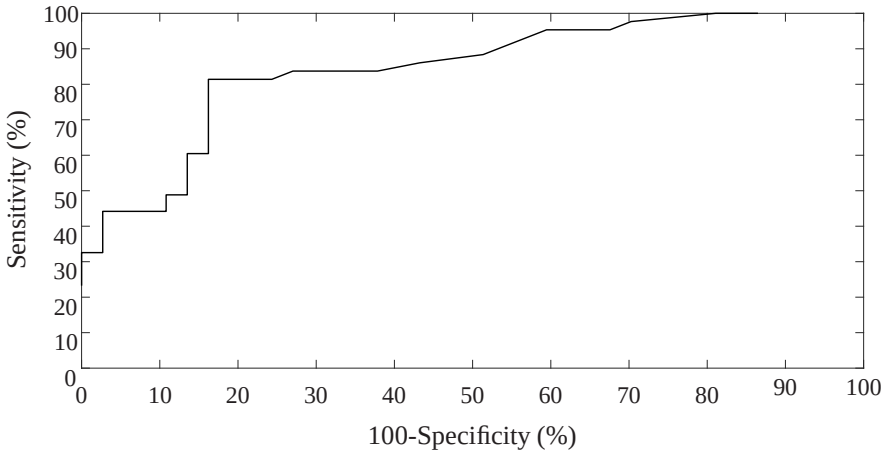

Figure 5: ROC curve for the selection of the threshold for alert generating.

threshold). As shown in the figure, window size $= 24$ hours presents the highest accuracy of 82.5% on the considered training set. These values are then considered for the following.

4.5. Performance Evaluation

After the illustration of the extraction and selection of the parameters, the model is tested on the test sets. In this section, results are obtained by a 5-fold cross validation repeated 10 times. Table 2 presents the performance of each added phase to obtain at the end the performance of the complete proposed model. The modeling of the data by associating and combining masses from all the parameters leads to a sensitivity of 70.23% and a specificity of 71.74% over the training sets and Se = 70.16% and Sp = 67.89% over the test sets. However, when the parameter selection phase was performed, an enhancement in the sensitivity was noted over the training sets (Se = 78.10%, Sp = 66.91%) and the test sets (Se = 72.59%, Sp = 61.16%). In addition, discounting the mass functions using the error rates improved the performance to 81.65% of sensitivity and 74.72% of specificity over the training sets and 77.24% and 71.25% for sensitivity and specificity respectively over the test sets. However, when the correlation was considered in the selection phase the performances decreased with $Se = 80.18\%$ and $Sp = 69.29\%$ over the training sets and 74.10%, 61.12% over the test sets.

4.6. Comparison to the state-of-the-art methods

The proposed model is compared to some classification techniques such as Bayesian hypothesis test, k-nearest neighbors (kNN) and SVM. The Bayesian hypothesis test is based on Bayes theorem. It is a probability model that consists of factorizing a joint probability distribution into a set of conditional distributions for each variable. The k-nearest neighbors is one of the basic algorithms in machine learning. It classifies a new observation to a class by choosing the majority class among the k nearest neighbors in

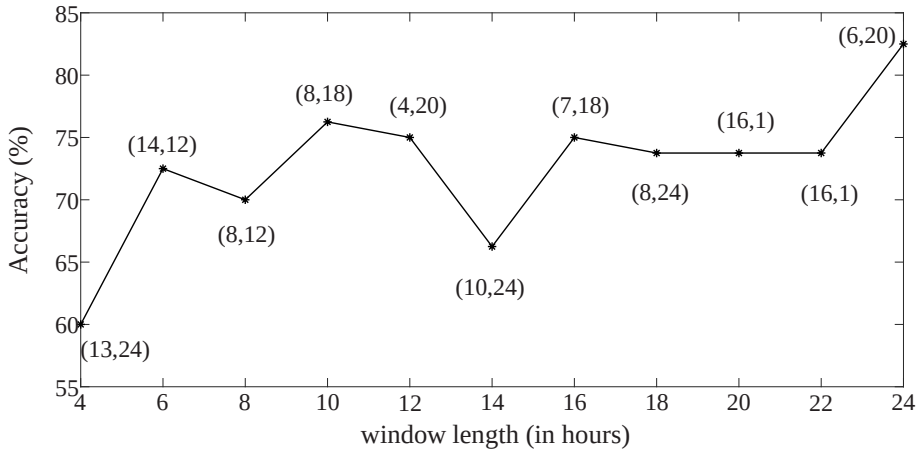

Figure 6: Changes in the accuracy over the training set with windows length. Values in the figure denote (number of parameters, threshold).

Table 2: Performance of the proposed model and the influence of each phase.

Method	**training set**		**test set**	
	Se(%)	Sp(%)	Se(%)	Sp(%)
BF without discounting, nor selection	70.23	71.74	70.16	67.89
BF without discounting	78.10	66.91	72.59	61.16
complete BF model	81.65	74.72	77.24	71.25
complete BF model+corr	80.18	69.29	74.10	61.12

the training set. A ten-fold cross validation was performed to obtain k that minimizes the test loss. The optimal k was found to be 8. As for SVM, it has proven to be a good model to classify data. It can be used to differentiate the data using a decision boundary that produces the optimal separation of classes. Table 3 shows the performance indexes of the proposed model compared to these described techniques. As shown, the proposed model outperforms the kNN, the SVM as well as the bayesian tests, that are a simplest form of the evidence theory where the ambiguities between the sets are not considered. These results show the importance of the proposed model.

Table 3: Comparison to state-of-the-art classification methods

Method	**Sensitivity (%)**	**Specificity (%)**
KNN	59.20	79.75
Bayesian test	67.74	65
SVM	58.67	74.06
The proposed Model	**77.24**	**71.25**

5. Discussion

This study proposed a real-time model, based on the belief functions theory, for predicting ARDS prior to its onset. ARDS results from inflammatory alveolar injury occurring progressively [46]. The process begins with the destruction of the barriers of the alveolar membranes resulting by increasing the alveolar permeability. Then, injuries progress causing decreased pulmonary compliance which leads to pulmonary hypertension and refractory hypoxia [47, 48]. Moreover, ARDS has been linked to clinical features such as severe dyspnea, tachypnea and hypoxemia according to [49]. Other studies on the clinical profile of ARDS had shown that it is associated with breathlessness, hypotension, tachypnea [50] and tachycardia [51]. Although, there are no clear clinical features for ARDS, it is evident that ARDS is linked to cardiorespiratory and cardiovascular mechanisms. Therefore, the four vital signs that are considered are the heart rate, the respiratory rate, the oxygen saturation and the mean airway blood pressure. However, there is a lack in the literature for the characterization of ARDS using feature extraction.

In feature extraction techniques, parameters are extracted from raw data signals and pertinent ones are selected to enhance the fusion performance. The characterization of signals using the extraction of parameters has been widely applied in biomedical applications. For instance, an analysis of heart rate variability during syncope was conducted by extracting parameters such as the mean, the standard deviation of the RR interval and non linear parameters such as the sample entropy and the detrended fluctuation analysis [52]. Moreover, linear and non-linear parameters were extracted from heart rate variability signals for ARDS subjects to analyze their response to alveolar recruitment manoeuver [53]. Only few studies have considered other cardiovascular signals than heart rate, like blood pressure and oxygen saturation signals [31, 54]. A characterization of heart beat and blood pressure for diabetes patients using time domain parameters such as the mean, the standard deviation, the skewness and the kurtosis was studied in [31]. In addition, detrended fluctuation analysis was extracted from blood pressure signal to study its dynamics through surgical procedure in rats [55]. In [33], a characterization of periventricular leukomalacia, a brain injury affecting infants, is proposed by extracting minimum, maximum, mean, variance, skewness, kurtosis, energy of wavelet coefficients and sample entropy from heart rate, mean arterial blood pressure and oxygen saturation. From what preceded, we can conclude that the extraction of parameters from different physiological signals might help in the characterization of physiological aspects related to several pathologies, such as ARDS.

Hence, in this paper, linear and non-linear parameters were extracted from the time series as mean, standard deviation, skewness, kurtosis, sample entropy and detrended fluctuation analysis. Linear parameters provide information regarding the distributions of the data. Distributions were shown to be asymmetric, having wide tails and being widely spread. This verifies that biomedical data are not gaussian [56]. Conversely, it was found that heart rate and respiratory rate had higher sample entropy in ARDS group, thus increased complexity [57]. However, oxygen saturation presented lower complexity in ARDS subjects. In other terms, SpO_2 presents more similarity in the data. From DFA_1 and DFA_2 values, we can notice that SpO_2 and MABP had lower correlations in ARDS subjects [36].

Moreover, feature fusion is performed using the belief functions framework. The proposed belief functions framework defines ARDS and non-ARDS groups based on the probability distributions of the data according to each parameter. In addition, these models consider supper subsets instead of considering only singletons subsets, thus they introduce the notion of ambiguity between choosing an ARDS or non-ARDS states. The belief theory also takes into account the reliability of each source of information presented by the discounting operation. The reliability of the sources is a very important characteristic, especially when working with parameters extracted from physiological signals. On top of these comes the importance of belief functions framework, that is the modeling of the data even with missing recordings. It often happens that some signals are missing in some part of the recordings because of disconnected electrodes or a sudden movement of the patient. Unlike classical data mining techniques, the belief functions guarantee that missing parameters due to missing signals will not affect the overall performance of features fusion.

From the results, the reduction of the number of parameters, by performing a selection procedure, improved the sensitivity of the model and reduced the complexity of the computations as well. This way only parameters having low error rates are included in the model and the combination that presents the best local accuracy is considered. Thus, the modeling of the data is done using the minimum amount of parameters instead of using all the extracted parameters. Then, the inclusion of the conditional reliability of each source has led to an enhancement in the accuracy of the model over the training and the test sets. Each parameter gives information regarding the patient and the reliability of the parameter itself in distinguishing between states. Finally, 77% of ARDS patients are correctly identified in real-time before the occurrence of ARDS and only 29% of non-ARDS patients are misclassified and considered as possible developers of ARDS. The obtained results demonstrate, beside the already existing studies on ARDS, that ARDS is linked to cardiorespiratory and cardiovascular mechanisms. More importantly, ARDS can be predicted using non-invasive physiological signals instead of using clinical exams or variables that necessitate the presence of subjects in hospitals for long period [15, 16, 14].

It is shown from the results that this model outperformed the classical classifiers tested similarly on the data. It is worth noting that the bayesian tests perform only on singletons and the state membership is determined by computing the likelihood ratio. However, the added ambiguity set in the proposed evidence-based model may affect the final decision since it is considered in both discounting and combination phases. Thus, the advantage of such models over the classical classifiers, especially the bayesian tests, is the inclusion of higher order sets that illustrate the ambiguity intervals.

Previous studies were conducted on the prediction of ARDS or the mortality related to ARDS using computed tomographic images [16] or clinical variables [15, 14], that necessitate clinical exams or the presence of subjects in the hospitals for long periods. However, the approach proposed in this paper uses only vital signs that can be collected using non-invasive techniques, thus without disturbing the subjects. Moreover, these studies present general statistical models to detect ARDS assuming that all subjects will present similar changes; while this approach is a subject-based one that considers an initial stable state for each subject and computes the ongoing parameters with respect to the stable state. In addition, an information fusion was handled using the evidence

theory to consider the ambiguity and unreliability of the sources. Finally, this approach achieved good performances for both sensitivity and specificity indexes for the real-time surveillance of ARDS.

6. Conclusion

This paper proposes an evidence-based model for the prediction of ARDS in intensive care unit patients. This work presents several contributions. Non invasive vital signs are included in the study for many reasons, the facility of their acquisition, the possible integration in home surveillance systems and the link between these signals and the risk factors associated with ARDS. Linear and non-linear parameters were computed and considered the source of information, since they can give information about the properties of a signal more than the signal itself. Imprecision and unreliability of information sources were considered by the belief functions model. It assigns masses to each subset computed from a predefined training set. Then, these masses were discounted and combined according to the reliability of each source of information. This model is then extended to reduce the dimension of the input by performing a parameter selection procedure. This model has achieved high performances in both ARDS and non-ARDS groups. In addition, it outperforms state of the art techniques. Further work must be done to extract more parameters that provide evidence on different characteristics in the signals. Moreover, it would be interesting to establish the relationships between the changes in time series and the cardiovascular mechanism. A further study on the parameters selection will also be done, to take into consideration the dependance of parameters from the beginning of the selection process.

Acknowledgment

The authors would like to thank Université de Technologie de Troyes, France and the Lebanese University, Lebanon for their funding of this research.

References

[1] United Nations, Department of Economic and Social Affairs, Population Division (2017), World Population Prospects: The 2017 Revision, Key Findings and Advance Tables, working Paper No. ESA/P/WP/248.

[2] M. J. Prince, F. Wu, Y. Guo, L. M. G. Robledo, M. O'Donnell, R. Sullivan, S. Yusuf, The burden of disease in older people and implications for health policy and practice, The Lancet 385 (9967) (2015) 549 – 562. doi:http://dx.doi.org/10.1016/S0140-6736(14)61347-7.

[3] S. L. Grace, G. Taherzadeh, I. S. J. Chang, J. Boger, A. Arcelus, S. Mak, C. Chessex, A. Mihailidis, Perceptions of seniors with heart failure regarding autonomous zero-effort monitoring of physiological parameters in the smart-home environment, Heart and Lung: The Journal of Acute and Critical Care 46 (4) (2017) 313 – 319.

[4] A. Lorenz, R. Oppermann, Mobile health monitoring for the elderly: Designing for diversity, Pervasive and Mobile Computing 5 (5) (2009) 478 – 495. doi:https://doi.org/10.1016/j.pmcj.2008.09.010.

[5] F. Sufi, Q. Fang, I. Khalil, S. S. Mahmoud, Novel methods of faster cardiovascular diagnosis in wireless telecardiology, IEEE Journal on Selected Areas in Communications 27 (4). doi:https://doi.org/10.1109/JSAC.2009.090515.

[6] A. R. M. Forkan, I. Khalil, A clinical decision-making mechanism for context-aware and patient-specific remote monitoring systems using the correlations of multiple vital signs, Computer Methods and Programs in Biomedicine 139 (2017) 1 – 16. doi:https://doi.org/10.1016/j.cmpb.2016.10.018.

[7] L. Ware, M. Matthay, The acute respiratory distress syndrome, New England Journal of Medicine 342 (18) (2000) 1334–1349.

[8] K. P. Steinberg, L. D. Hudson, R. B. Goodman, C. L. Hough, P. N. Lanken, R. Hyzy, B. T. Thompson, M. Ancukiewicz, National Heart, Lung, and Blood Institute, Acute Respiratory Distress Syndrome (ARDS) Clinical Trials Network, Efficacy and Safety of Corticosteroids for Persistent Acute Respiratory Distress Syndrome, NEJM 354 (16) (2006) 1671–1684. doi:10.1056/NEJMoa051693.

[9] D. G. Ashbaugh, D. B. Bigelow, T. Petty, B. Levine, Acute Respiratory Distress in Adults, The Lancet 290 (7511) (1967) 319–323. doi:10.1016/S0140-6736(67)90168-7.

[10] G. R. Bernard, A. Artigas, K. Brigham, J. Carlet, K. Falke, L. Hudson, M. Lamy, J. Legall, A. Morris, R. Spragg, The American-European Consensus Conference on ARDS. Definitions, mechanisms, relevant outcomes, and clinical trial coordination., AJRCCM 149 (1994) 818–824. doi:10.1164/ajrccm.149.3.7509706.

[11] V. M. Ranieri, G. D. Rubenfeld, B. Thompson, N. Ferquson, E. Caldwell, E. Fan, L. Camporota, A. Slutsky, Acute Respiratory Distress Syndrome: The Berlin Definition, Jama 307 (23) (2012) 2526–2533. doi:10.1001/jama.2012.5669.

[12] S. Yu, D. C. Christiani, B. T. Thompson, E. K. Bajwa, M. N. Gong, Role of diabetes in the development of acute respiratory distress syndrome., CCM Journal 41 (12) (2013) 2720–2732. doi:10.1097/CCM.0b013e318298a2eb.

[13] G. Singh, G. Gladdy, T. Chandy, N. Sen, Incidence and outcome of acute lung injury and acute respiratory distress syndrome in the surgical intensive care unit., IJCCM 18 (10) (2014) 659–665. doi:10.4103/0972-5229.142175.

[14] C. M. Ennett, K. P. Lee, L. J. Eshelman, B. Gross, L. Nielsen, J. J. Frassica, M. Saeed, Predicting respiratory instability in the ICU, in: 30th Int. Conf. of the IEEE EMBS., IEEE, Vancouver, British Columbia, Canada, 2008, pp. 2848–2851. doi:10.1109/IEMBS.2008.4649796.

[15] P. Navarrete-Navarro, M. Ruiz-Bailén, R. Riviera-Fernandez, F. Guerrero-Lopez, M. D. P.-G. de Guzman, G. Vazquez-Mata, Acute respiratory distress syndrome in trauma patients: Icu mortality and prediction factors, ICM Journal 26 (11) (2000) 1624–1629. doi:10.1007/s001340000683.

[16] K. Ichikado, M. Suga, Y. Gushima, H. Miyakawa, M. Tsubamoto, T. Johkoh, N. Hirata, T. Yoshinaga, Y. Kinoshita, Y. Yamashita, Y. Sasaki, Prediction of prognosis for acute respiratory distress syndrome with thin-section ct: Validation in 44 cases 1, Radiology 238 (1) (2006) 321–329.

[17] H. Ravishankar, A. Saha, G. Swamy, S. Genc, An early respiratory distress detection method with Markov models, in: 36th Int. Conf. of the IEEE EMBS., IEEE, Chicago, Illinois, USA, 2014, pp. 3438–3441. doi:10.1109/EMBC.2014.6944362.

[18] C. Velardo, S. A. Shah, O. Gibson, H. Rutter, A. Farmer, L. Tarassenko, Automatic generation of personalised alert thresholds for patients with COPD, in: 2nd EUSIPCO, IEEE, Lisbon, Portugal, 2014, pp. 1990–1994.

[19] I. Yoo, P. Alafaireet, M. Marinov, K. Pena-Hernandez, R. Gopidi, J.-F. Chang, L. Hua, Data mining in healthcare and biomedicine: A survey of the literature, Journal of Medical Systems 36 (4) (2012) 2431–2448. doi:10.1007/s10916-011-9710-5.

[20] Y. ler, M. Kuntalp, Combining classical hrv indices with wavelet entropy measures improves to performance in diagnosing congestive heart failure, Computers in Biology and Medicine 37 (10) (2007) 1502 – 1510. doi:https://doi.org/10.1016/j.compbiomed.2007.01.012.

[21] M. Seera, C. P. Lim, W. S. Liew, E. Lim, C. K. Loo, Classification of electrocardiogram and auscultatory blood pressure signals using machine learning models, Expert Systems with Applications 42 (7) (2015) 3643 – 3652. doi:https://doi.org/10.1016/j.eswa.2014.12.023.

[22] L. Clifton, D. A. Clifton, P. J. Watkinson, L. Tarassenko, Identification of patient deterioration in vital-sign data using one-class support vector machines, in: Computer Science and Information Systems (FedCSIS), 2011 Federated Conference on, IEEE, 2011, pp. 125–131.

[23] M. S. Jassas, A. A. Qasem, Q. H. Mahmoud, A smart system connecting e-health sensors and the cloud, in: 2015 IEEE 28th Canadian Conference on Electrical and Computer Engineering (CCECE), 2015, pp. 712–716. doi:10.1109/CCECE.2015.7129362.

[24] L. Fang, X. Chen, Z. Fang, K. Tong, J. Liu, Z. He, J. Li, Multi-parameter health monitoring watch, in: 2017 IEEE 19th International Conference on e-Health Networking, Applications and Services (Healthcom), 2017, pp. 1–6. doi:10.1109/HealthCom.2017.8210807.

[25] T. Klingeberg, M. Schilling, Mobile wearable device for long term monitoring of vital signs, Computer Methods and Programs in Biomedicine 106 (2) (2012) 89 – 96, design of Environments for Ageing. doi:https://doi.org/10.1016/j.cmpb.2011.12.009.

[26] A. L. Goldberger, L. A. N. Amaral, L. Glass, J. M. Hausdorff, P. C. Ivanov, R. G. Mark, J. E. Mietus, PhysioBank, PhysioToolkit, and PhysioNet : Components of a New Research Resource for Complex Physiologic Signals, Circulation 101 (23) (2000) e215–e220. doi:10.1161/01.CIR.101.23.e215.

[27] M. Saeed, M. Villarroel, A. T. Reisner, G. Clifford, L.-W. Lehman, G. Moody, T. Heldt, T. H. Kyaw, B. Moody, R. G. Mark, Multiparameter Intelligent Monitoring in Intensive Care II (MIMIC- II): A public-access intensive care unit database, CCM Journal 39 (5) (2011) 952–960. doi:10.1097/CCM.0b013e31820a92c6.Multiparameter.

[28] J. Shao, Linear model selection by cross-validation, Journal of the American Statistical Association 88 (422) (1993) 486–494. doi:10.1080/01621459.1993.10476299.

[29] A. Camm, M. Malik, J. Bigger, G. Breithardt, S. Cerutti, R. Cohen, P. Coumel, E. Fallen, H. Kennedy, R. Kleiger, et al., Heart rate variability: standards of measurement, physiological interpretation and clinical use. task force of the european society of cardiology and the north american society of pacing and electrophysiology, Circulation 93 (5) (1996) 1043–1065.

[30] A. Bauer, J. W. Kantelhardt, P. Barthel, R. Schneider, T. Mäkikallio, K. Ulm, K. Hnatkova, A. Schömig, H. Huikuri, A. Bunde, et al., Deceleration capacity of heart rate as a predictor of mortality after myocardial infarction: cohort study, The lancet 367 (9523) (2006) 1674–1681.

[31] A. L. Rivera, B. Estañol, H. Sentíes-Madrid, R. Fossion, J. C. Toledo-Roy, J. Mendoza-Temis, I. O. Morales, E. Landa, A. Robles-Cabrera, R. Moreno, et al., Heart rate and systolic blood pressure variability in the time domain in patients with recent and long-standing diabetes mellitus, PloS one 11 (2) (2016) e0148378.

[32] J. R. Moorman, J. B. Delos, A. A. Flower, H. Cao, B. P. Kovatchev, J. S. Richman, D. E. Lake, Cardiovascular oscillations at the bedside: early diagnosis of neonatal sepsis using heart rate characteristics monitoring, Physiological measurement 32 (11) (2011) 1821.

[33] A. Jalali, D. J. Licht, C. Nataraj, Discovering hidden relationships in physiological signals for prediction of periventricular leukomalacia, in: 2013 35th Annual International Conference of the IEEE Engineering in Medicine and Biology Society (EMBC), IEEE, 2013, pp. 7080–7083.

[34] D. E. Lake, J. S. Richman, M. P. Griffin, J. R. Moorman, Sample entropy analysis of neonatal heart rate variability, Am. J. Physiol. Regul. Integr. Comp. Physiol. 283 (2002) 789–797.

[35] D. P. Francis, K. Willson, P. Georgiadou, R. Wensel, L. C. Davies, A. Coats, M. Piepoli, Physiological basis of fractal complexity properties of heart rate variability, man J. Physiol. 542 (2002) 619–629.

[36] C.-K. Peng, S. Havlin, H. E. Stanley, A. L. Goldberger, Quantification of scaling exponents and crossover phenomena in nonstationary heartbeat time series, Chaos: An Interdisciplinary Journal of Nonlinear Science 5 (1) (1995) 82–87.

[37] P. Millar, A. Levy, C. McGowan, N. McCartney, M. MacDonald, Isometric handgrip training lowers blood pressure and increases heart rate complexity in medicated hypertensive patients, Scandinavian journal of medicine & science in sports 23 (5) (2013) 620–626.

[38] A. P. Dempster, Upper and lower probabilities induced by a multivalued mapping, The annals of mathematical statistics 83 (1967) 325–339.

[39] G. Shafer, A mathematical theory of evidence, Vol. 1, Princeton university press, Princeton, 1976.

[40] P. Smets, R. Kennes, The transferable belief model, Artificial Intelligence 66 (2) (1994) 191 – 234. doi:https://doi.org/10.1016/0004-3702(94)90026-4.

[41] P. Smets, Belief function: the disjunctive rule of combination and the generalized bayesian theorem, International Journal of Approximate Reasoning 9 (1) (1993) 1 – 35.

[42] D. Mercier, E. Lefèvre, F. Delmotte, Belief functions contextual discounting and canonical decompositions, International Journal of Approximate Reasoning 53 (2) (2012) 146 – 158.

[43] D. Mercier, F. Pichon, E. Lefèvre, Corrigendum to belief functions contextual discounting and canonical decompositions [international journal of approximate reasoning 53 (2012) 146-158], International Journal of Approximate Reasoning 70 (2016) 137 – 139.

[44] P. A. Devijver, J. Kittler, Pattern recognition: A statistical approach, Prentice hall, 1982.

[45] G. Fele-Žorž, G. Kavšek, Ž. Novak-Antolič, F. Jager, A comparison of various linear and non-linear signal processing techniques to separate uterine emg records of term and preterm delivery groups, Medical & biological engineering & computing 46 (9) (2008) 911–922.

[46] A. W. Thille, A. Esteban, P. Fernández-Segoviano, J.-M. Rodriguez, J.-A. Aramburu, P. Vargas-Errázuriz, A. Martín-Pellicer, J. A. Lorente, F. Frutos-Vivar, Chronology of histological lesions in acute respiratory distress syndrome with diffuse alveolar damage: a prospective cohort study of clinical autopsies, The lancet Respiratory medicine 1 (5) (2013) 395–401.

[47] R. Mac Sweeney, D. F. McAuley, Acute respiratory distress syndrome, The Lancet 388 (10058) (2016) 2416–2430.

[48] N. Patroniti, S. Isgrò, A. Zanella, Clinical management of severely hypoxemic patients, Current opinion in critical care 17 (1) (2011) 50–56.

[49] O. Gajic, O. Dabbagh, P. K. Park, A. Adesanya, S. Y. Chang, P. Hou, I. Harry Anderson, J. J. Hoth, M. E. Mikkelsen, N. T. Gentile, M. N. Gong, D. Talmor, E. Bajwa, T. R. Watkins, E. Festic, M. Yilmaz, R. Iscimen, D. A. Kaufman, A. M. Esper, R. Sadikot, I. Douglas, J. Sevransky, , M. M. on behalf of the U.S. Critical Illness, I. T. G. L. I. P. S. I. (USCIITGLIPS), Early identification of patients at risk of acute lung injury: evaluation of lung injury prediction score in a multicenter cohort study, American Journal of Respiratory and Critical Care Medicine 183 (4) (2011) 462–470.

[50] D. Chaudhury, J. Hasan, S. Paul, I. Ali, A study on clinical profile and outcome of patients with acute respiratory distress syndrome in a tertiary care hospital in north east india, Sepsis 13 (2017) 29–5.

[51] P. K. Park, J. W. Cannon, W. Ye, L. H. Blackbourne, J. B. Holcomb, W. Beninati, L. M. Napolitano, Incidence, risk factors, and mortality associated with acute respiratory distress syndrome in combat casualty care, Journal of Trauma and Acute Care Surgery 81 (5) (2016) S150–S156.

[52] N. Khodor, D. Matelot, G. Carrault, H. Amoud, M. Khalil, N. Ville, F. Carre, A. Hernandez, Kernel based support vector machine for the early detection of syncope during head-up tilt test, Physiological measurement 35 (10) (2014) 2119.

[53] A. Borghi-Silva, G. R. das Chagas, V. M. Borges, M. S. Reis, E. M. de Carvalho, Analysis of heart rate variability and cardiovascular response in the alveolar recruitment manoeuver in acute respiratory distress syndrome, Journal of Respiratory and CardioVascular Physical Therapy 3 (2) (2016) 30–39.

[54] Z. Turianikova, K. Javorka, M. Baumert, A. Calkovska, M. Javorka, The effect of orthostatic stress on multiscale entropy of heart rate and blood pressure, Physiological measurement 32 (9) (2011) 1425.

[55] C. Galhardo, T. Penna, M. A. de Menezes, P. Soares, Detrended fluctuation analysis of a systolic blood pressure control loop, New Journal of Physics 11 (10) (2009) 103005.

[56] K. C. Chua, V. Chandran, U. R. Acharya, C. M. Lim, Application of higher order statistics/spectra in biomedical signalsa review, Medical engineering & physics 32 (7) (2010) 679–689.

[57] J. S. Richman, J. R. Moorman, Physiological time-series analysis using approximate entropy and sample entropy, American Journal of Physiology-Heart and Circulatory Physiology 278 (6) (2000) H2039–H2049.